Optics Letters

High-resolution ghost imaging through complex scattering media via a temporal correction

Yin Xiao,[1] Lina Zhou,[1] and Wen Chen[1,2,*]

[1]Department of Electronic and Information Engineering, The Hong Kong Polytechnic University, Hong Kong, China
[2]Photonics Research Institute, The Hong Kong Polytechnic University, Hong Kong, China
*Corresponding author: owen.chen@polyu.edu.hk

Received 12 May 2022; revised 26 June 2022; accepted 30 June 2022; posted 1 July 2022; published 19 July 2022

In this Letter, we propose high-resolution ghost imaging (GI) through complex scattering media using temporal correction. We provide evidence that the theoretical description about GI based on spatially correlated beams is still incomplete and cannot work in complex scenarios. We complete the description of temporal correction of beam correlations in GI. The optical experiments demonstrate that high-resolution ghost images can always be retrieved by using the rectified temporally corrected beam correlation algorithm even in complex, dynamic, and highly strong scattering environments where conventional GI cannot work. By using the proposed method, the quality of the retrieved ghost images through complex scattering media can be enhanced effectively as the number of realizations increases, which cannot be achieved by conventional GI. The established general framework provides optical insights beyond the current understanding of GI, and the rectified theory and experimental results would represent a key step toward applications of GI over a wide range of free-space wave propagation environments.

https://doi.org/10.1364/OL.463897

Ghost imaging (GI) was studied and applied to retrieve sample information based on spatially correlated beams [1]. In GI, the illumination beam is split into two beam paths. One beam illuminates a sample collected by using a single-pixel bucket detector (BD) without spatial resolution, and the transverse distribution of another beam that never interacts with the sample is collected by using a pixelated detector. Spatial properties of the sample can be retrieved using a correlation operation between the spatially correlated beams. There is either quantum or classical correlation involved in GI [2]. In quantum optics, GI is created with correlated beams of entangled photons and is developed based on quantum entanglement proposed by Klyshko *et al*. [3]. In Ref. [4], Shih *et al*. developed GI using entanglement photon pairs generated from spontaneous parametric downconversion. Although quantum-entanglement-based GI has been theoretically and experimentally verified, it was found that quantum entanglement was not a prerequisite to retrieve ghost images. Therefore, classical GI using pseudo-thermal light has been further developed [5].

In GI, different light sources have been studied and applied, e.g., x ray [6], Terahertz [7], cold atom [8], electron [9], and neutron [10]. The extension and studies are significant for the development of GI. For instance, x-ray GI could reduce the dose rate of radiation used in imaging and tomography [11]. Computational GI (CGI) [12] has also been developed which simplifies the GI setup with only one beam path by explicitly controlling the distribution of incident illumination using a spatial light modulator (SLM).

GI could outperform 2D pixelated-detector-based imaging approaches in many situations, e.g., absorbing samples [13], low light intensities [14], and scattering media [15]. The GI method has been employed in various fields, e.g., 3D imaging [16], cytometry [17], encryption [18], telecommunications [19], remote sensing [20], and pattern recognition [21]. The modified GI algorithms [22,23] have also been studied and applied for the purpose of finding novel applications and retrieving ghost images with improved signal-to-noise ratio (SNR). Although a second-order correlation algorithm has been investigated in GI, it is not a complete theoretical description. In the optical channel of GI, scaling factors exist physically and can play an important role. GI based on spatially correlated beams always considers scaling factors as a constant, which may not be fully feasible. The second-order correlation algorithm is not generally feasible and efficient for GI to work in various free-space wave propagation environments, and it is always desirable to complete the theoretical description of GI in order to establish a general framework.

In this Letter, we propose high-resolution temporally corrected GI (TCGI) through complex scattering media. We provide evidence that the theoretical description about GI based on spatially correlated beams is still incomplete and cannot work in complex scenarios. We complete the description of the temporal correction of beam correlations in GI. The proposed TCGI scheme takes scaling factors into consideration, and a theoretical derivation about GI is completely described. In the proposed TCGI scheme, a temporal carrier is introduced and used to correct scaling factors physically existing in the imaging channel. High-resolution ghost images can always be retrieved by using the proposed TCGI scheme even in complex, dynamic, and highly strong scattering environments where conventional GI cannot work. The rectified correlation algorithm in the proposed TCGI scheme provides a general framework and optical insights beyond the current understanding of GI and gives rise to applications of GI over a wide range of free-space wave propagation environments.

When scaling factors physically existing in GI are taken into consideration, the single-pixel detection process in various free-space wave propagation environments in GI can be described by

$$B = k \int I(\mathbf{x})G(\mathbf{x})d\mathbf{x}, \tag{1}$$

where B denotes the single-pixel value (i.e., a realization in GI), k denotes the scaling factor in optical channel, $I(\mathbf{x})$ denotes an illumination pattern with spatial coordinate $\mathbf{x}$, and $G(\mathbf{x})$ denotes the intensity transmission function of a sample. Then, the correlation operation between intensity fluctuation δB and $\delta I(\mathbf{x})$ can be described by

$$\begin{aligned} O(\mathbf{x}) &= \langle \delta B \delta I(\mathbf{x}) \rangle \\ &= \langle (B - \langle B \rangle)\,(I(\mathbf{x}) - \langle I(\mathbf{x}) \rangle) \rangle\,, \end{aligned} \tag{2}$$

where $O(\mathbf{x})$ denotes a retrieved ghost image, $\langle\rangle$ denotes an ensemble averaging over the total number of realizations, $\delta B = B - \langle B \rangle$, and $\delta I(\mathbf{x}) = I(\mathbf{x}) - \langle I(\mathbf{x}) \rangle$.

The scaling factors physically existing in GI are always assumed as constant which has no effect on the correlation algorithm in Eq. (2). Since complex and dynamic factors, such as scattering or turbulence, are a significant challenge in GI, scaling factors in the optical channel could be severely modified. A direct calculation of $\langle B \rangle$ and δB could be physically meaningless due to the variation of scaling factors, e.g., through dynamic and strong scattering media. Therefore, the correlation algorithm is not generally feasible and effective for the retrieval of ghost images in many application scenarios. It is crucial to investigate the variation of scaling factors physically existing in the optical channel and completely derive a second-order correlation algorithm to establish a general framework for GI.

To solve the problem induced by the variation of scaling factors physically existing in GI, a temporal carrier $T(\mathbf{x})$ is introduced (see Section 1 in Supplement 1 for details) in this study and used before each illumination pattern $I(\mathbf{x})$. When the fixed temporal carrier and each illumination pattern are alternately used to sequentially illuminate a sample in GI, the single-pixel detection process is respectively described by

$$B_{ti} = k_{ti} \int T(\mathbf{x})G(\mathbf{x})d\mathbf{x}, \tag{3}$$

$$B_i = k_i \int I_i(\mathbf{x})G(\mathbf{x})d\mathbf{x}, \tag{4}$$

where i denotes a sequence (i.e., 1,2,3,...), B_{ti} denotes the single-pixel intensity values corresponding to the temporal carrier $T(\mathbf{x})$, k_{ti} denotes scaling factors corresponding to the temporal carrier, B_i denotes the single-pixel intensity value corresponding to each illumination pattern $I_i(\mathbf{x})$, and k_i denotes scaling factors corresponding to the illumination patterns. Since the time interval between the fixed temporal carrier $T(\mathbf{x})$ and each illumination pattern $I_i(\mathbf{x})$ embedded into an SLM is short, a relationship of $k_{ti} \approx k_i$ can be employed. Therefore, scaling factors in GI can be eliminated by using the recorded single-pixel intensity values corresponding to the temporal carrier, which is described by

$$\frac{B_i}{B_{ti}} \approx \frac{\int I_i(\mathbf{x})G(\mathbf{x})d\mathbf{x}}{\int T(\mathbf{x})G(\mathbf{x})d\mathbf{x}}. \tag{5}$$

Here, a fixed temporal carrier $T(\mathbf{x})$ is used before each illumination pattern $I_i(\mathbf{x})$. The denominator in Eq. (5) can be considered as a constant ρ described by

$$\rho = \int T(\mathbf{x})G(\mathbf{x})d\mathbf{x}. \tag{6}$$

Then, we have

$$\int I_i(\mathbf{x})G(\mathbf{x})d\mathbf{x} \approx \rho \frac{B_i}{B_{ti}}. \tag{7}$$

The left-hand side in Eq. (7) represents the sum of a product between each illumination pattern $I_i(\mathbf{x})$ and intensity transmission function of the sample. After $\int I_i(\mathbf{x})G(\mathbf{x})\,d\mathbf{x}$ is denoted as B_i', we have

$$B_i' \approx \rho \frac{B_i}{B_{ti}}. \tag{8}$$

Unlike the resultant B in Eq. (1), B_i' in Eq. (8) does not contain the impact of scaling factors physically existing in the optical channel of GI. The result obtained in Eq. (8) is further used in the correlation algorithm, and a wide range of free-space wave propagation environments, e.g., through complex, dynamic, and highly strong scattering media, can be studied. Applying Eq. (8) into Eq. (2), we have

$$O(\mathbf{x}) = \left\langle \left(\rho \frac{B_i}{B_{ti}} - \left\langle \rho \frac{B_i}{B_{ti}} \right\rangle \right) (I_i(\mathbf{x}) - \langle I_i(\mathbf{x}) \rangle) \right\rangle. \tag{9}$$

Since ρ is a constant that has no effect, it can be omitted. Equation (9) can be re-written as

$$O(\mathbf{x}) = \left\langle \left(\frac{B_i}{B_{ti}} - \left\langle \frac{B_i}{B_{ti}} \right\rangle \right) (I_i(\mathbf{x}) - \langle I_i(\mathbf{x}) \rangle) \right\rangle. \tag{10}$$

The rectified correlation algorithm in Eqs. (9) and (10) provides a general framework for GI and can be used for the retrieval of high-resolution ghost images in various free-space wave propagation environments, e.g., imaging without scattering media in free space, and through complex and dynamic scattering media where conventional GI methods cannot work.

To verify the rectified correlation algorithm in the proposed TCGI scheme, a series of optical experiments are conducted to realize the retrieval of high-resolution ghost images in complex scenarios. In Fig. 1, a green laser with power of 25.0 mW and wavelength of 532.0 nm is used. A series of 2D random amplitude-only patterns with 128×128 pixels are generated and sequentially embedded into an amplitude-only SLM (Holoeye, LC-R720) with pixel size of 20.0 μm. The fixed temporal carrier and each illumination pattern are alternately embedded into

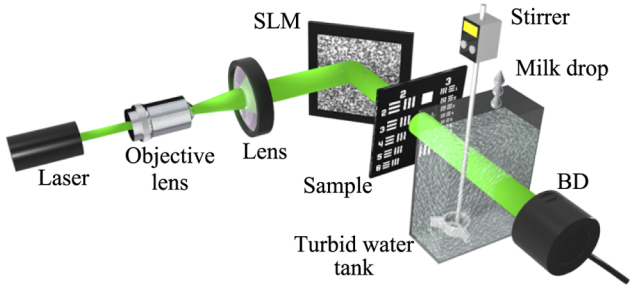

Fig. 1. Schematic of an optical setup in complex, dynamic, and highly strong scattering media to verify the rectified correlation algorithm in the proposed TCGI scheme. SLM: Spatial light modulator; BD: Bucket detector. A USAF 1951 resolution target is used as a sample.

(a) (b) (c)

Fig. 2. (a) Ground truth (i.e., the part inside red box), (b) a retrieved ghost image using GI with 38,000 realizations, and (c) a retrieved ghost image using the rectified correlation algorithm in the proposed TCGI scheme with 38,000 realizations. The retrieved ghost image is slightly tilted due to the illumination angle.

the amplitude-only SLM. As a typical example, 38,000 random amplitude-only illumination patterns are used in this study and the fixed temporal carrier, i.e., a pre-generated random amplitude-only pattern, is used before each illumination pattern. A USAF 1951 resolution target is used as a sample in the experimental setup, and imaging through complex, dynamic, and highly strong scattering media is studied. It is worth noting that the amplitude-only patterns are projected onto the sample by using a 4*f* system, which is not shown in Fig. 1. In the water tank (transparent polymethyl methacrylate), with dimensions of 10.0 cm (L) × 30.0 cm (W) × 30.0 cm (H), 6000 ml of clean water is first placed. Then, in the imaging process, skimmed milk (total volume of 10.0 ml) keeps dropping into the water tank over 102.0 minutes. To create a dynamic environment, a stirrer is used to operate at 500.0 rpm. A single-pixel BD (Thorlabs, PDA100A2) is used to record a series of intensity values. In optical experiments, the axial distance between the water tank and single-pixel detector is 22.0 cm, and the axial distance between the sample and single-pixel detector is 42.0 cm.

The free-space wave propagation environment in Fig. 1 changes the characteristics of the optical channel in the single-pixel measurement process. Suppose that only the realizations corresponding to the series of illumination patterns are used based on spatially correlated beams in Eq. (2), it is impossible to retrieve the information of the sample. The ground truth is shown inside a red box in Fig. 2(a), and the retrieved result based on Eq. (2) is shown in Fig. 2(b). It can be seen in Fig. 2(b) that no information about the sample can be retrieved, even when 38,000 realizations are used. Experimental results demonstrate that the theoretical description of GI is incomplete and cannot provide a general framework for the retrieval of ghost images in various free-space wave propagation environments. When the realizations measured corresponding to the series of illumination patterns and the fixed temporal carrier are employed in Eq. (10) in the proposed TCGI scheme, the experimental result is shown in Fig. 2(c). It can be seen that a high-resolution ghost image is retrieved, and a spatial resolution of 70.15 μm (i.e., element 6 of group 2 in the USAF 1951 resolution target) is achieved. The spatial resolution achieved is close to the theoretical limit in this GI system. Experimental results in Fig. 2 verify the rectified correlation algorithm in the proposed TCGI scheme.

The retrieved ghost images are also evaluated by using the SNR [24]. Figure 3 shows SNR values of the retrieved ghost images with a different number of realizations in conventional GI and the proposed TCGI scheme, when a complex and dynamic environment in Fig. 1 is studied. It is shown in Fig. 3 that

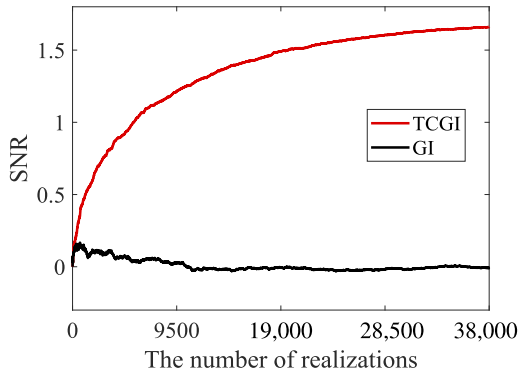

Fig. 3. Relationships between the different number of realizations and SNR values of the retrieved sample images. Conventional GI and the proposed TCGI schemes are tested, when the scattering media in Fig. 1 is used.

SNR values of the retrieved ghost images in the proposed TCGI scheme increase correspondingly as the number of realizations increases, and the SNR value can achieve up to 1.70. In contrast, SNR values of the retrieved ghost images in conventional GI are always close to 0 even with a large number of realizations. It is experimentally demonstrated that the theory rectified here for GI removes the effect of the physically existing scaling factors via temporal correction and provides a framework for the retrieval of high-resolution ghost images in various free-space wave propagation environments.

In addition to conventional GI, modified GI reconstruction algorithms, i.e., differential GI (DGI) [22] and normalized GI (NGI) [23], also cannot retrieve any information about the sample, and experimental results are obtained (see Fig. S2 in Supplement 1). DGI and NGI were developed to enhance the quality of retrieved ghost images but these approaches cannot work when the scattering environment in Fig. 1 is studied. The experimental results of DGI and NGI are similar to those obtained by using conventional GI: no information about the sample can be retrieved in DGI and NGI. This shows again that the theoretical description about GI based on spatially correlated beams is still incomplete. Furthermore, the fundamental principle in the proposed TCGI scheme is completely different from that in NGI where the recorded single-pixel intensity value is divided by a reference value R_i, i.e., $R_i = \int I_i(\mathbf{x})d\mathbf{x}$. It can be seen that the parameters B_{ti} in Eq. (3) and R_i are different. The parameter B_{ti} denotes an interaction between the temporal carrier and intensity transmission function of the sample, and R_i denotes only the sum of each illumination pattern. NGI was developed to enhance the quality of the retrieved ghost images based on Eq. (2), and TCGI is proposed in this study to complete a theoretical description of spatially correlated beams and establish a general framework for GI which can give rise to applications in various free-space wave propagation environments, e.g., high-resolution imaging through complex and dynamic scattering media.

Visualization 1, Visualization 2, Visualization 3, Visualization 4 further illustrate the different GI algorithms (GI, DGI, NGI, and TCGI, respectively) in a complex, dynamic, and highly strong scattering environment. It is demonstrated that the quality of the ghost images retrieved based on the rectified theory in the proposed TCGI scheme is high, and conventional GI theories (i.e., GI, DGI and NGI) cannot retrieve any information about the sample.

In addition, performance of the total variation regularization algorithm (i.e., TVAL3 [25]) through complex scattering media is also discussed (see Fig. S3 in Supplement 1). The results demonstrate advantages of the proposed TCGI method in complex scattering media.

Based on the experimental setup in Fig. 1, it is also feasible to retrieve high-resolution ghost images in the proposed TCGI scheme when there is no turbid water tank in free space (see Fig. S4 in Supplement 1), and a comparison among different methods (i.e., GI, DGI, NGI, TVAL3, and TCGI) in free space without scattering media [26] is also conducted (see Fig. S5 in Supplement 1). It can be seen in the experimental results that the proposed TCGI method can also obtain a better recovery result compared with the other methods.

In recent years, deep learning has become a powerful tool for imaging through complex scattering media [27–29]. Unlike data-driven or model-driven algorithms, the proposed TCGI scheme provides a general framework for imaging through complex scattering media. More discussions of the proposed TCGI method can be found in Section 6 of Supplement 1.

In conclusion, we have provided evidence that the theoretical description of GI based on spatially correlated beams is still incomplete and cannot work in complex scenarios. The theoretical description of temporal correction of beam correlations in GI is completed and reported here. Characteristics of the optical channel have been taken into consideration, and a correlation algorithm in GI is rectified to be applicable in a wide range of free-space wave propagation environments. The theory we rectified can establish a general framework to provide optical insights beyond the current understanding of GI and can eliminate the influence of physically existing scaling factors via temporal correction. By using the proposed TCGI scheme, high-resolution optical imaging through complex scattering media is realized, and the quality of the recovered ghosts through complex scattering media can be enhanced effectively when the number of realizations increases. A new avenue can be opened up for the application of GI.

Funding. Basic and Applied Basic Research Foundation of Guangdong Province (2022A1515011858); Hong Kong Research Grants Council (15224921, C5011-19G); Hong Kong Polytechnic University (1-BD4Q, 1-W19E).

Disclosures. The authors declare no conflicts of interest.

Data availability. Data underlying the results presented in this paper are not publicly available at this time but may be obtained from the authors upon reasonable request.

Supplemental document. See Supplement 1 for supporting content.

REFERENCES

1. B. I. Erkmen and J. H. Shapiro, Adv. Opt. Photonics **2**, 405 (2010).
2. J. H. Shapiro and R. W. Boyd, Quantum Inf. Process. **11**, 949 (2012).
3. D. N. Klyshko, Sov. Phys. JETP **67**, 1131 (1988).
4. D. V. Strekalov, A. V. Sergienko, D. N. Klyshko, and Y. H. Shih, Phys. Rev. Lett. **74**, 3600 (1995).
5. R. S. Bennink, S. J. Bentley, and R. W. Boyd, Phys. Rev. Lett. **89**, 113601 (2002).
6. D. Pelliccia, A. Rack, M. Scheel, V. Cantelli, and D. M. Paganin, Phys. Rev. Lett. **117**, 113902 (2016).
7. C. M. Watts, D. Shrekenhamer, J. Montoya, G. Lipworth, J. Hunt, T. Sleasman, S. Krishna, D. R. Smith, and W. J. Padilla, Nat. Photonics **8**, 605 (2014).
8. R. I. Khakimov, B. M. Henson, D. K. Shin, S. S. Hodgman, R. G. Dall, K. G. H. Baldwin, and A. G. Truscott, Nature **540**, 100 (2016).
9. S. Li, F. Cropp, K. Kabra, T. J. Lane, G. Wetzstein, P. Musumeci, and D. Ratner, Phys. Rev. Lett. **121**, 114801 (2018).
10. Y. H. He, Y. Y. Huang, Z. R. Zeng, Y. F. Li, J. H. Tan, L. M. Chen, L. A. Wu, M. F. Li, B. G. Quan, S. L. Wang, and T. J. Liang, Sci. Bull. **66**, 133 (2021).
11. A. X. Zhang, Y. H. He, L. A. Wu, L. M. Chen, and B. B. Wang, Optica **5**, 374 (2018).
12. J. H. Shapiro, Phys. Rev. A **78**, 061802 (2008).
13. G. Brida, M. Genovese, and I. R. Berchera, Nat. Photonics **4**, 227 (2010).
14. P. A. Morris, R. S. Aspden, J. E. C. Bell, R. W. Boyd, and M. J. Padgett, Nat. Commun. **6**, 5913 (2015).
15. A. M. Paniagua-Diaz, I. Starshynov, N. Fayard, A. Goetschy, R. Pierrat, R. Carminati, and J. Bertolotti, Optica **6**, 460 (2019).
16. B. Q. Sun, M. P. Edgar, R. Bowman, L. E. Vittert, S. Welsh, A. Bowman, and M. J. Padgett, Science **340**, 844 (2013).
17. S. Ota, R. Horisaki, Y. Kawamura, M. Ugawa, I. Sato, K. Hashimoto, R. Kamesawa, K. Setoyama, S. Yamaguchi, K. Fujiu, K. Waki, and H. Noji, Science **360**, 1246 (2018).
18. W. Chen, B. Javidi, and X. Chen, Adv. Opt. Photonics **6**, 120 (2014).
19. P. Ryczkowski, M. Barbier, A. T. Friberg, J. M. Dudley, and G. Genty, Nat. Photonics **10**, 167 (2016).
20. B. I. Erkmen, J. Opt. Soc. Am. A **29**, 782 (2012).
21. X. D. Qiu, D. K. Zhang, W. H. Zhang, and L. X. Chen, Phys. Rev. Lett. **122**, 123901 (2019).
22. F. Ferri, D. Magatti, L. A. Lugiato, and A. Gatti, Phys. Rev. Lett. **104**, 253603 (2010).
23. B. Q. Sun, S. S. Welsh, M. P. Edgar, J. H. Shapiro, and M. J. Padgett, Opt. Express **20**, 16892 (2012).
24. B. Redding, M. A. Choma, and H. Cao, Nat. Photonics **6**, 355 (2012).
25. C. Li, W. Yin, H. Jiang, and Y. Zhang, Comput. Optim. Appl. **56**, 507 (2013).
26. Z. Cai, J. W. Chen, G. Pedrini, W. Osten, X. Liu, and X. Peng, Light: Sci. Appl. **9**, 143 (2020).
27. M. Lyu, H. Wang, G. Li, S. Zheng, and G. Situ, Adv. Photonics **1**, 036002 (2019).
28. E. Guo, S. Zhu, Y. Sun, L. Bai, C. Zuo, and J. Han, Opt. Express **28**, 2433 (2020).
29. Y. Sun, J. Shi, L. Sun, J. Fan, and G. Zeng, Opt. Express **27**, 16032 (2019).